

See discussions, stats, and author profiles for this publication at: <https://www.researchgate.net/publication/51031803>

Gas-Phase Fragmentation of $[M + nH + OH]^{n+}$ Ions Formed from Peptides Containing Intra-Molecular Disulfide Bonds

ARTICLE in JOURNAL OF THE AMERICAN SOCIETY FOR MASS SPECTROMETRY · MAY 2011

Impact Factor: 2.95 · DOI: 10.1007/s13361-011-0104-1 · Source: PubMed

CITATIONS

12

READS

35

4 AUTHORS, INCLUDING:



Xiaoxiao Ma

Purdue University

16 PUBLICATIONS 340 CITATIONS

SEE PROFILE



Chasity B Love

Purdue University

2 PUBLICATIONS 20 CITATIONS

SEE PROFILE



Xinrong Zhang

Tsinghua University

188 PUBLICATIONS 6,897 CITATIONS

SEE PROFILE



RESEARCH ARTICLE

Gas-Phase Fragmentation of $[M + nH + OH]^{n+}$ Ions Formed from Peptides Containing Intra-Molecular Disulfide Bonds

Xiaoxiao Ma,^{1,2} Chasity B. Love,² Xinrong Zhang,¹ Yu Xia²¹Department of Chemistry, Tsinghua University, Beijing, People's Republic of China²Department of Chemistry, Purdue University, West Lafayette, IN 47907-1393, USA

Abstract

In this study, we systematically investigated gas-phase fragmentation behavior of $[M + nH + OH]^{n+}$ ions formed from peptides containing intra-molecular disulfide bond. Backbone fragmentation and radical initiated neutral losses were observed as the two competing processes upon low energy collision-induced dissociation (CID). Their relative contribution was found to be affected by the charge state (n) of $[M + nH + OH]^{n+}$ ions and the means for activation, i.e., beam-type CID or ion trap CID. Radical initiated neutral losses were promoted in ion-trap CID and for lower charge states where mobile protons were limited. Beam-type CID and dissociation of higher charge states of $[M + nH + OH]^{n+}$ ions generally gave abundant backbone fragmentation, which was highly desirable for characterizing peptides containing disulfide bonds. The amount of sequence information obtained from CID of $[M + nH + OH]^{n+}$ ions was compared with that from CID of disulfide bond reduced peptides. For the 11 peptides studied herein, similar extent of sequence information was obtained from these two methods.

Key words: Gas phase ion/radical reaction, Intra-molecular disulfide bond, Collision induced dissociation, Peptide sequencing, Tandem mass spectrometry

Introduction

Disulfide bond formation is one type of post-translational modifications (PTMs) and is responsible for the stabilization of the native structures of proteins [1]. Although collision-induced dissociation (CID) has been successfully and widely used for peptide/protein identification, very limited sequence information is obtained from peptides or proteins containing intra-molecular disulfide bonds [2]. The difficulty stems from the fact that two bonds need to be broken to form one sequence ion within the peptide backbone area covered by the disulfide bond, which

is not always accessible under low energy CID conditions. In addition, peptide backbone is more readily cleaved than the disulfide bonds for peptides having mobile protons [3]. Consequently, the major backbone fragments are due to cleavages of exocyclic amide bonds, and very little structural information within the disulfide loop can be acquired.

The most widely used approach in the analysis of disulfide peptides involves reduction of disulfide linkages followed by alkylation in solution before tandem mass spectrometry analysis. Rich sequence information can often be obtained from the reduced peptides. If disulfide bonds are not highly intertwined, their connecting patterns can be speculated by comparing the CID spectrum of the reduced peptide to that of the intact peptide [2]. Methods have also been developed to cleave disulfide bonds in the gas phase. Preferential cleavage of disulfide bonds over peptide backbone under CID conditions is observed for deprotonated

Electronic supplementary material The online version of this article (doi:10.1007/s13361-011-0104-1) contains supplementary material, which is available to authorized users.

Correspondence to: Yu Xia; e-mail: yxia@purdue.edu

Received: 29 December 2010
Revised: 4 February 2011
Accepted: 9 February 2011
Published online: 23 March 2011

peptides [4, 5], peptide ions having limited mobile protons [6, 7], and metal cationized peptide ions [3, 8–10]. Electron detachment dissociation (EDD) induces selective S–S or C–S cleavages for peptide anions [11]. Ultraviolet photon dissociation (UVPD) at 157 nm cleaves disulfide bonds with high specificity via electronic excitation [12]. In electron capture dissociation (ECD) [13] and electron transfer dissociation (ETD) [14, 15], disulfide bond cleavage is observed as a competitive process to backbone fragmentation. In addition, cleavage of both disulfide bond and peptide backbone can result from a single electron transfer event, providing sequence information within the disulfide linkage [16].

Recently, our group reported the observation of disulfide bond cleavage when peptide ions generated from nano-electrospray (nanoESI) were allowed to interact with a low-temperature plasma (LTP) before entering a mass spectrometer [17]. Sulfenyl radical ($-\text{SO}\cdot$) and sulfhydryl ($-\text{SH}$) were formed at the cleavage site and a reaction pathway involving dissociative $\text{OH}\cdot$ addition to the disulfide bond was proposed (Scheme 1). The definitive picture of the proposed mechanism, however, needs further validation by conducting gas-phase ion/radical reactions with isolated reaction species. In general, chain separation was observed for peptides containing an inter-molecular disulfide bond, while the OH adduct ($[\text{M} + \text{OH} + n\text{H}]^{n++}$) was one of the main products for peptides containing intra-molecular disulfide bonds. Subsequent CID of $[\text{M} + \text{OH} + n\text{H}]^{n++}$ ions produced peptide backbone fragmentation at sites that were originally protected by the disulfide linkage, demonstrating that the disulfide bond was already cleaved. As a consequence, significantly improved sequence information was obtained for peptides containing one or multiple disulfide bonds [17].

The OH adduct of a protonated peptide, i.e., $[\text{M} + \text{OH} + n\text{H}]^{n++}$, is an odd electron ion. Although gas-phase chemistry of protonated peptide ions has been widely studied, the knowledge on peptide radical ions is relatively limited [18]. Typically, peptide radical ions cannot be formed directly and, therefore, indirect approaches are taken. Several research groups use the strategy of generating hydrogen deficient radical cations from CID of complexes between a transition metal and a peptide [19, 20], dissociation of noncovalent peptide complexes [21], and homolytic cleavages of amino acid residues modified with covalent bonds [22–25]. Hydrogen deficient peptide radical anions can be produced from EDD of deprotonated peptides [26, 27] or dissociation of negatively charged peptide–metal complexes [28]. Given the coexistence of charges and radical sites in peptide/protein radical ions, radical-initiated reactions compete with charge-directed pathways upon their dissociation. The relative contributions of these two pathways

are affected by many factors, including the amino acid composition of the peptide and how the radical sites are formed [21, 28–30]. Hydrogen rich peptide radical cations ($[\text{M} + n\text{H}]^{(n-1)+\cdot}$) are generated in ECD and ETD processes, which subsequently fragment at N–C α bonds to form c- and z-types of ions [31–33]. The fragmentation mechanisms for both processes are still under debate and subjected to experimental and theoretical studies [34–36].

Herein, we systematically investigate low energy collisional activation of $[\text{M} + n\text{H} + \text{OH}]^{n++}$ ions generated from peptides containing single intra-molecular disulfide bond. From this study, we hope to gain a better understanding on the interplay between the radical-initiated and charge-directed processes upon the dissociation of peptide radical ions and also to find conditions that the amount of structural information can be maximized for characterizing disulfide peptides.

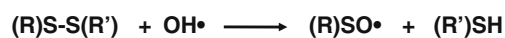
Experimental

Materials

Endotoxin inhibitor, IGF-I analog and TGF α (34–43) (rat) were purchased from Bachem (Torrance, CA, USA). All the other peptides were purchased from AnaSpec (Fremont, CA, USA). The names and sequences of these peptides are listed in Table 1. All samples, unless otherwise noted, were used without further purification. Reduced peptides were generated by mixing 10 μL peptide solution (1 mg/mL in water) with 10 times molar excess of 1 mg/mL dithiothreitol solution (DTT, Sigma-Aldrich, St. Louis, MO, USA). The pH of the solution was adjusted to 8.5 through the addition of ammonium hydroxide, and the final solution was allowed to react in room temperature for 30 min. The working solutions of all peptides were prepared to a final concentration of 10 μM in 49.5/49.5/1 (vol/vol/vol) methanol/water/acetic acid.

Ionization and Reaction

The experimental setup is shown in Figure 1a. Peptide ions were generated by nanoelectrospray ionization (nanoESI) in positive ion mode. The nanoESI tips were pulled from borosilicate glass capillaries (1.5 mm o.d. and 0.86 mm i.d.) using a P97 Flaming/Brown micropipette puller (Sutter Instruments, Novato, CA, USA). Peptide solution was loaded from the back of the nanoESI tip. A stainless steel wire was inserted into the tip to ensure electric contact with the solution. The nanoESI emitter was inserted into the main arm of a T-shaped tube and was kept in line with the inlet of the mass spectrometer at a distance of 8–10 mm. A low temperature helium plasma was initiated in the side arm of the T-shape tube to form hydroxyl radicals as described previously [17]. The nanoESI plume of peptides was allowed to interact with hydroxyl radicals and the products formed in situ were analyzed on-line by mass spectrometry.



Scheme 1. Proposed mechanism for the dissociation of a disulfide bond

Table 1. List of Peptides Containing One Intra-Molecular Disulfide Bond Used in This Study

Label	Sequence	Name
1	CHSGYVGVR	TGF α (34-43) (rat)
2	CYAAPLKPAKSC	IGF-I analog
3	CIELLQARC	Selectin binding peptide
4	CGRRAGGSC	Cancer related IL-11R α binding peptide
5	CNGRC-NH ₂	NGR, peptide 3
6	CGNKRTRGC	LyP-1, peptide 1
7	CLPTRHMAC	CD154 blocking peptide
8	CSRNLIDC	PDGF-BB peptide fragment
9	AGCKNFFWKFTSC	Somatostatin-14
10	CTTHWGFTLC	CTT, gelatinase inhibitor
11	KTKCKFLKKC	Endotoxin inhibitor

Mass Spectrometry

Unless otherwise mentioned, mass spectra were collected on a 4000QTRAP tandem mass spectrometer (Applied Biosystems/SCIEX, Toronto, Canada), which has a triple

quadrupole/linear ion trap configuration [37]. Two types of collisional activation methods are available on this instrument, i.e., beam-type CID and ion trap CID. In beam-type CID, the precursor ions are isolated by Q1 quadrupole array and accelerated to Q2 for collisional activation. The collision energy (CE) was optimized for each spectrum and was generally within the range of 12–60 V. Ion trap CID was conducted in Q3 linear ion trap, where a dipolar excitation was used for collisional activation. The activation amplitudes were within the range of 20–60 (arbitrary unit). Instrument control, data acquisition, and processing were carried out using Analyst 1.5 software. The typical parameters of the mass spectrometer used in this study were set as follows: spray voltage, 1200–1800 V; curtain gas, 10; declustering potential, 20 V. Mass analysis was achieved by using Q3 as a linear ion trap. A scan rate of 1000 Da/s was typically used. To acquire mass spectra with higher resolution, scan rate at 250 Da/s was used. Data shown here were typically a averages of 50 scans. Accurate mass measurement was obtained on an LTQ-Orbitrap (Thermo Fisher Scientific, San Jose, CA, USA) with an external calibration and the mass resolution was set at 60,000.

Results and Discussion

Formation of $[M + nH + OH]^{n++}$ Ions

The low temperature helium plasma can function as a source for hydroxyl radicals when there is trace water and oxygen around [38]. The interaction between nanoESI plume of the peptide solution and hydroxyl radicals was enabled in a T-shaped tube and the reaction products were analyzed on-line using mass spectrometry as shown in Figure 1a. Dissociative addition of the hydroxyl radical to a disulfide bond within peptide ions is observed as one of the main reaction pathways, while oxidation of the amino acid residue side chains can be competitive when the concentration of hydroxyl radicals are relatively high [17]. The experimental conditions in the source region were tuned so that the OH adduct was formed as a major product compared with side-chain oxidation. Figure 1b shows a typical reaction mass spectrum for a peptide containing an intra-molecular disulfide bond (Peptide 4, CGRRAGGSC, 1-9 disulfide linkage) when the nanoESI source and the LTP are operating simultaneously. The OH adduct of the peptide ($[M + nH + OH]^{n++}$) can be clearly detected as well as side chain oxidation product ions ($[M + nH + mO]^{n++}$). In most conditions, $[M + nH + OH]^{n++}$ ions could be well isolated and they were subjected to either beam-type or ion trap collisional activation.

Figure 2a shows an example of beam-type CID mass spectrum of isolated $[M + 2H + OH]^{2++}$ ions derived from Peptide 7 (CLPTRHMAC, 1-9 disulfide linkage). A series of peaks corresponding to peptide backbone fragments, i.e., b and y ions, can be clearly observed. These ions have a mass increase either 1 or 16 Da higher than the predicted fragment ions formed from the same peptide with the disulfide bond homolytically cleaved, i.e., •S-CLPTRHMAC-S•. Since no

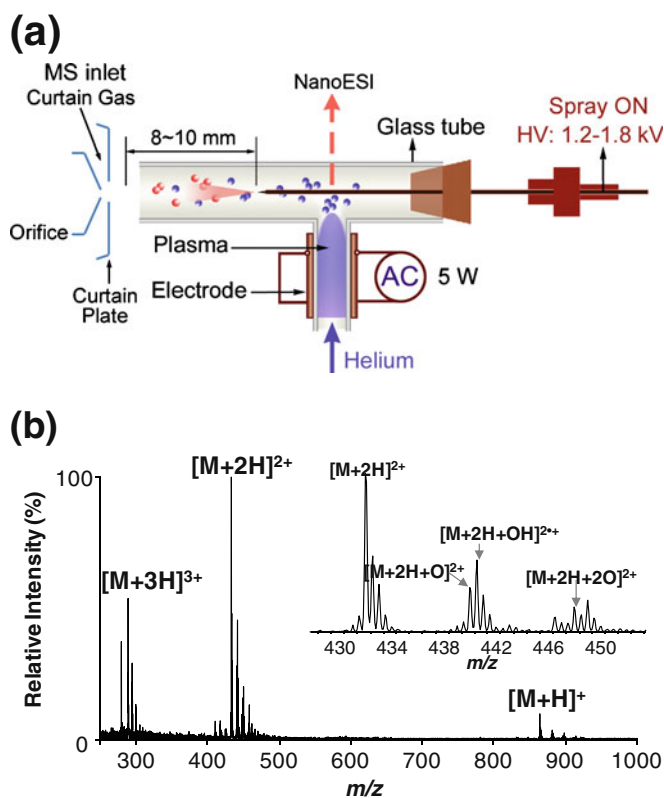


Figure 1. (a) Schematic diagram of the experimental setup allowing for interactions between hydroxyl radicals and peptide ions and (b) nanoESI mass spectrum of Peptide 4 (CGRRAGGSC, 1-9 disulfide linkage) when the helium LTP source was operating. The inset shows a magnified view of the doubly charged peptide ion region

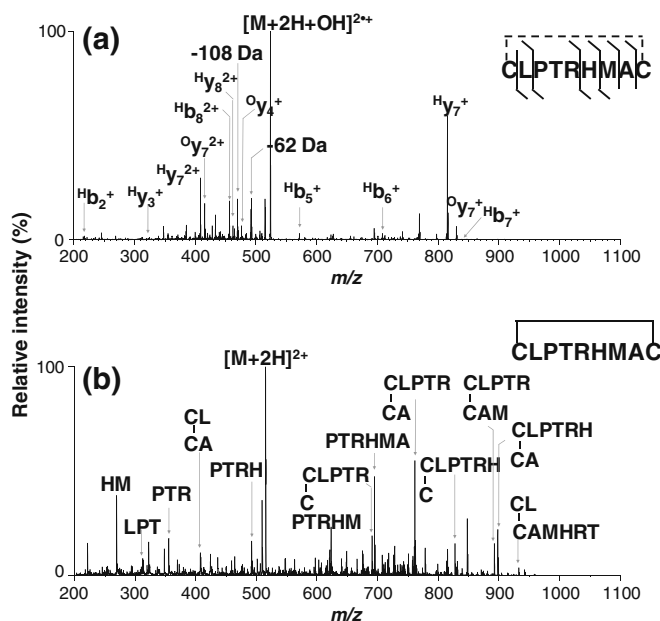


Figure 2. MS² beam-type CID of (a) $[M + OH + 2H]^{2+}$ (CE: 25 V) and (b) intact peptide ions, $[M + 2H]^{2+}$ (CE: 28 V) derived from Peptide 7 (CLPTRAHMAC, 1-9 disulfide linkage)

fragment ion with a mass increase of 17 Da was observed, the O and H atoms should add separately to each sulfur atom of the disulfide bond as indicated in Scheme 1. These mass shifts are also reflected in the fragment ion nomenclature. For instance, H_{y_m} means the y_m ion has a mass increase due to the addition of H, and O_{b_n} indicates the b_n ion has an O addition. Due to the cleavage of the disulfide bond, the subsequent CID produces rich backbone fragmentation. In Figure 2a, sequence ions including $H_{b_2}^+$, $H_{b_5}^+$, $H_{b_6}^+$, $H_{y_3}^{2+}$, $O_{y_4}^{2+}$, $H_{y_7}^+$, and $O_{y_7}^+$ can be clearly identified, which count for six out of eight possible amide bond cleavages. Other than backbone fragments, there are peaks corresponding to neutral losses of 62 and 108 Da. They originate from radical-initiated processes and are discussed in detail below. Figure 2b shows CID data of intact Peptide 7 ions ($[M + 2H]^{2+}$). Many peaks are internal fragments formed from cleavages of two amide bonds with the disulfide bond remaining intact. This observation is consistent with existing studies that higher energy is required to break a disulfide bond within the peptide ions when there are mobile protons [39]. Due to the complexity of the spectrum, obtaining sequence information directly from CID of the intact disulfide peptide is challenging.

Neutral Losses

Unique neutral losses such as losses of 62, 95, and 108 Da were consistently observed from CID of $[M + OH + nH]^{n+}$ ions for all the disulfide peptides studied herein. In order to understand the origin of these losses, tandem mass spectrometry and accurate mass measurement were employed.

Figure 3a shows MS² ion trap CID of $[M + OH + H]^{+}$ derived from Peptide 5 (CNGRC-NH₂, 1-5 disulfide linkage). The dominant fragments are due to losses of 61.9819, 94.9613, and 107.9689 Da, corresponding to elemental composition of CH₂SO (61.9826 Da), CH₃SO (94.9625 Da), and C₂H₄S₂O (107.9704 Da), respectively. When the 62 Da neutral loss peak ($[M + OH + H - 62]^{+}$) was further subjected to ion trap CID, 32.9795 and 45.9871 Da were observed as the dominant fragments (Figure 3b) and they were likely to have elemental compositions of HS (32.9799 Da) and CH₂S (45.9877 Da). The data from Figure 3 are highly suggestive that neutral losses of 95 and 108 Da from $[M + OH + H]^{+}$ ions result from sequential losses, i.e., loss of 62 Da (CH₂SO) followed by a loss of either 33 Da (HS) or 46 Da (CH₂S).

Tentative fragmentation pathways for the above neutral losses are proposed in Scheme 2. The 62 Da (CH₂SO) loss is due to β -cleavage to sulfenyl radical (-SO•) formed at the cysteine sulfur. The same loss has been observed in CID of O_{y_n} and O_{b_n} ions before [17]. After loss of CH₂SO, a radical site is formed at the α -carbon of the cysteine residue. It has been observed that α -carbon radical formed in ECD and ETD processes migrates to other α -carbons or side-chain positions via fast intra-molecular hydrogen transfer [40] and initiates backbone or side-chain fragmentation, which is remote from the initial radical site [41, 42]. It is very likely that the α -carbon radical formed at one cysteine residue site

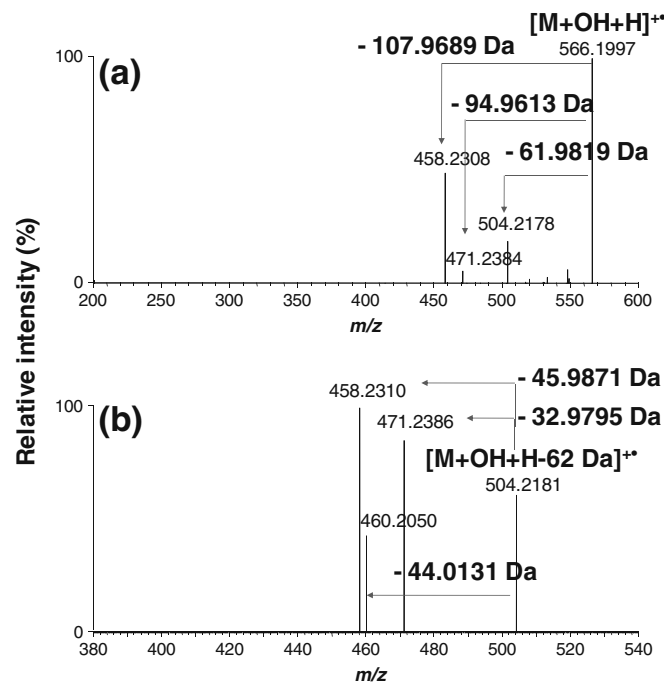
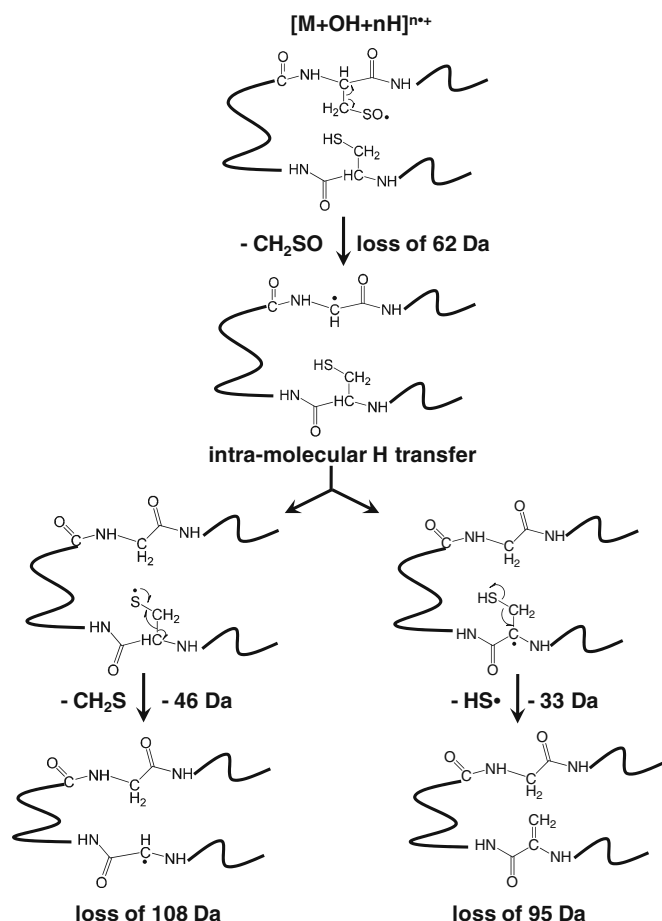


Figure 3. (a) MS² ion trap CID mass spectrum of $[M + OH + H]^{+}$ (Peptide 5, CNGRC-NH₂, 1-5 disulfide linkage) showing the dominant peaks due to neutral losses; (b) MS³ ion trap CID mass spectrum of $[M + OH + H - 62]^{+}$, isolated from (a)



Scheme 2. Possible fragmentation pathways for neutral losses of 62, 95, and 108 Da from CID of $[M + OH + nH]^{n++}$ ions

migrates to the sulfur atom or the α -carbon of the other cysteine residue upon collisional activation in this case. The following β -cleavage to the sulfur radical gives rise to CH_2S loss, while β -cleavage to the α -carbon radical generates $HS\bullet$ loss. Note that same losses from the cysteine residue have been observed from CID of z_n^{++} ions [43, 44] and hydrogen deficient peptide radical ions [21].

MS^3 of O-Addition Fragment Ions

CID of $[M + nH + OH]^{n++}$ gives rise to $^O b$ and $^O y$ ions which are also radical ions. Tandem mass spectrometry was applied to these ions to gain insight on their structures and the mobility of radical sites. The O-addition fragment ions derived from Peptides 1, 3, and 9 were selected as representative cases to show their fragmentation chemistry under collisional activation. MS^3 CID mass spectra of singly charged $^O y_4$ ions derived from Peptide 1 and singly charged $^O b_5$ ions derived from Peptide 3 are shown in Figure 4a and b, respectively. In both cases, the most abundant fragment ions are those due to radical initiated reactions, such as neutral losses of 62 or 49 Da [17]. Backbone fragmenta-

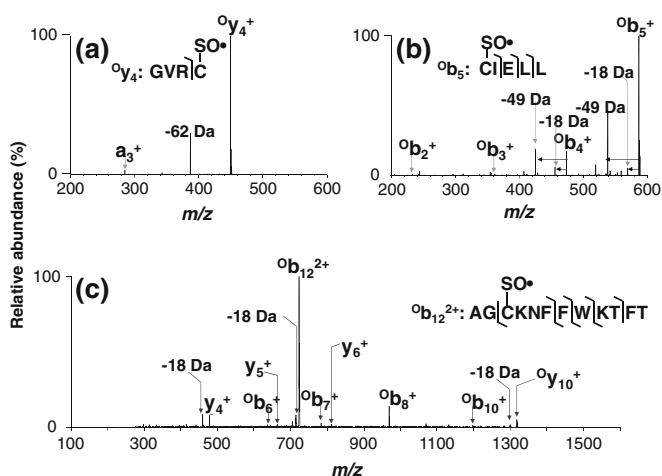


Figure 4. MS^3 CID mass spectrum of (a) $^O y_4^+$ ions derived from Peptide 1 (CHSGYVGVR, 1-10 disulfide linkage); (b) $^O b_5^+$ ions derived from Peptide 3 (CIELLQARC, 1-9 disulfide linkage), and (c) $^O b_{12}^{2+}$ ions derived from Peptide 9 (AGCKNFFWKTFTSC, 3-14 disulfide linkage). Nomenclature of the fragment ions generated in MS^3 is based on the sequence of the corresponding precursor ions

tion was also observed, such as a_3 from CID of $^O y_4$ ions (the fragment nomenclature is based on the sequence of $^O y_4$ ions), and $^O b_n$ ($n=2, 3, 4$) from CID of $^O b_5$ ions. For Peptide 9, doubly charged $^O b_{12}$ ions were isolated and further fragmented. Backbone fragments, including y_n ($n=4, 5, 6$) ions, $^O y_{10}$ ion, and $^O b_n$ ($n=6, 7, 8, 10$) ions were observed. To unambiguously assign the location of O attachment, a complete series of sequence ions containing the modification site needs to be observed. Although limited sequence fragments were observed for the three cases, the data were highly suggestive that oxygen was attached to the cysteine residue and did not move along the peptide chain under ion trap CID conditions. Note that this phenomenon is distinct from CID of $[M + OH + H-62]^{++}$ ions, where migration of the radical site was observed. The differences may be a result of different stability of sulfenyl radical and α -carbon radical.

Beam-Type and Ion-Trap CID of $[M + nH + OH]^{n++}$ Ions

The 4000Qtrap mass spectrometer provides two ways of performing low energy collisional activation, i.e., beam-type CID and ion trap CID. Beam-type CID is accomplished by accelerating ions of interest into the collision cell (Q2, ~ 8 mTorr), where they collide with the target nitrogen gas, while ion-trap CID is performed in the low pressure Q3 linear ion trap ($\sim 3 \times 10^{-5}$ Torr), where a dipolar ac is applied to resonantly excite the ions [37]. The two methods are similar in the way that multiple low energy collisions are responsible for activation. However, higher collisional energies (tens of eV/charge) and shorter activation time (10^{-4} s) are typically associated with beam-

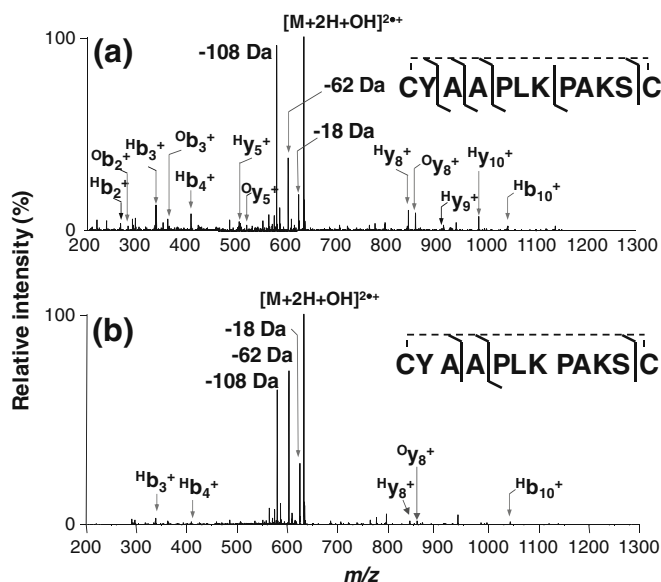


Figure 5. MS² CID mass spectrum of $[M + OH + 2H]^{2+}$ from Peptide 2 (CYAAPLPAKSC, 1-12 disulfide linkage): **(a)** beam-type CID, CE: 30 V and **(b)** ion trap CID, AF2: 60, excitation time: 100 ms

type CID as compared to ion trap CID [45]. Figure 5 shows beam-type CID and ion trap CID of $[M + nH + OH]^{n+}$ formed from Peptide 2 (CYAAPLPAKSC, 1-12 disulfide linkage). The two spectra are similar in that same major fragment ions, including both backbone fragments and neutral losses, can be found in both spectra. However, more backbone fragments are identified in beam-type CID, and their relative intensities are much higher than that of their counterparts in ion trap CID. For example, Hb_2^+ , Ob_2^+ , Ob_3^+ , Hy_5^+ , Oy_5^+ , Hy_9^+ , Hy_{10}^+ , and Hb_{10}^+ ions can only be detected in beam-type CID. Neutral losses, such as the losses of 18, 62, 95, and 108 Da from $[M + nH + OH]^{n+}$ ions, on the other hand, are more prominent in ion trap CID. Note that other than the loss of 18 Da (H_2O loss), the losses of 62, 95, and 108 Da all result from radical-initiated fragmentation as proposed in Scheme 2. Given that the lowest energy fragmentation pathways are preferred in ion trap CID due to its slow heating nature [46], observing abundant neutral losses in ion-trap CID is not surprising. The peptide backbone fragmentations, on the other hand, are typically charge directed even electron processes and are likely associated with higher activation energies [47]. Since higher collision energies can be accessed in beam-type CID, backbone fragmentation pathways can be more competitive. For all the disulfide peptides studied herein, it is consistently observed that backbone fragmentation is favored in beam-type CID, while neutral losses are more abundant in ion trap CID of $[M + nH + OH]^{n+}$ ions. From the perspective of peptide identification, beam-type CID of higher charge states of $[M + nH + OH]^{n+}$ ions is highly preferred.

Influence of Charge State on CID of $[M + nH + OH]^{n+}$ Ions

The charge states of an ion can greatly impact its gas-phase fragmentation chemistry. This phenomenon is well studied for protonated peptides and explained by the “mobile proton” model [48]. We are interested in understanding how charge state affects CID of $[M + nH + OH]^{n+}$ ions, given the possible competition between charge-directed and radical-directed fragmentation pathways. Figure 6 compares beam-type CID of triply, doubly, and singly charged $[M + nH + OH]^{n+}$ ions derived from Peptide 1 (CHSGYGVRC, 1-10 disulfide linkage). For the triply charged ions (Figure 6a), collision activation produces mostly backbone fragments, including Hy_4^+ , Oy_4^+ , Hb_5^+ , Ob_5^+ , Hb_6^+ , and Ob_6^+ . Since the first ¹³C isotopic peak of $[M + 3H + O]^{3+}$ is isobaric to $[M + 3H + OH]^{3+}$ and could not be isolated from each other, loss of valine from $[M + 3H + O]^{3+}$ was also observed ($[M - V + 2H + O]^{2+}$). Collisional activation of $[M + 2H + OH]^{2+}$ also produces abundant backbone fragmentation, as evidenced by a series sequence ions including Hb_n^+ ($n=2-4$), Ob_n^+ , Hy_n^+ ($n=2, 3$), and Oy_n^+ ($n=3, 4$). Losses of 62 and 108 Da are observed with significant intensities as well. In the CID mass spectrum of singly charged precursor ions, neutral losses (17, 18, 49, 62, 95, and 108 Da)

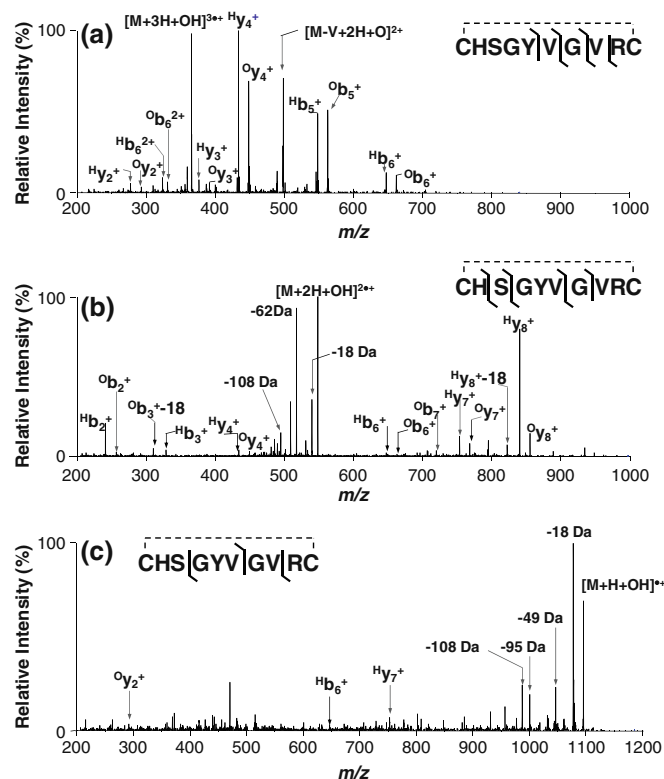


Figure 6. Beam-type CID mass spectra of **(a)** triply charged, **(b)** doubly charged, and **(c)** singly charged $[M + OH + nH]^{n+}$ ions formed from Peptide 1 (CHSGYGVRC, 1-10 disulfide linkage)

become the dominant fragments while only three tiny backbone fragments are observed (Oy_2 , Hb_6 , and Hy_7).

The abundant backbone fragmentation observed from higher charge states of $[M + nH + OH]^{n+}$ ions can be explained within the context of “mobile proton” model [48]. For most protonated peptides, backbone fragmentation is associated with a proton at the cleavage site. The protons that are not sequestered by arginine residues (mobile protons) can effectively reduce the activation energy for peptide backbone fragmentation and make the process more favorable than others [48]. Peptide 1 has one arginine in its sequence and there is no mobile proton in the singly charged precursor ions. Consequently, backbone fragmentation is barely observed, while ions generated by radical-initiated neutral losses and some other facile neutral losses are more abundant. For doubly and triply charged precursor ions, backbone fragmentation becomes dominant due to the presence of one and two mobile protons.

The influence of charge state on peptide backbone fragmentation from CID of $[M + nH + OH]^{n+}$ ions, reflected by the percentage of observed amide bond cleavages out of all possible ones (backbone frag%), is summarized in Table 2. For Peptides 3–8, there is no mobile proton in their lowest charge states (right column) and, therefore, the backbone frag% is rather low (0%–30%). However, in their highest charge states (left column), one mobile proton is present, leading to considerably improved backbone frag% (71%–100%). An exception is that the backbone frag% of triply charged Peptide 4 is only 25%, which is still an improvement compared with no backbone fragmentation observed in the lower charge states (2+ and 1+). Peptides 2 and 9 contain two lysine residues and no arginine residue.

Since the energy for proton “mobilization” is lower for lysine-containing peptides [48], the differences between the degree of backbone fragmentation for 3+ and 2+ charge states are less significant.

Comparisons to CID of Reduced Peptide

When the optimized collisional activation condition, i.e., beam-type CID of relatively high charge states is applied to $[M + nH + OH]^{n+}$ ions, rich sequence information can be obtained for peptides containing intra-molecular disulfide bonds. In order to evaluate its potential in analytical application, we further compared the above method to CID of disulfide bond reduced peptide ions ($[red - M + nH]^{n+}$), which is widely used for characterizing disulfide peptides. Peptide 9 (somatostatin) was used as an example to allow comparisons between the two methods. It is evident from the data in Figure 7 that the CID spectrum of $[M + 3H + OH]^{3+}$ is similar to that of the reduced peptide ions ($[red - M + 3H]^{3+}$, Figure 7b) in terms of fragment ion identities and their relative intensities. This similarity is likely attributed to the fact that the disulfide bond is already cleaved and proton directed backbone fragmentation is a favorable process in both cases. The main difference between the two spectra is that doublet peaks with a mass difference of 15 Da are often observed from CID of $[M + nH + OH]^{n+}$ due to the random attachment of O and H to either side of the disulfide bond to form $^Oy_n/^Hy_n$ or $^Ob_n/^Hb_n$ ion pairs. This feature does make the spectrum more complicated than that of the reduced peptide ions. Nevertheless, since the doublets are only observed for backbone fragmentation within the disulfide bond loop, those ions can be used to confirm the location of the disulfide bond. For

Table 2. Effect of Charge States on Backbone Fragmentation* of Peptides (Beam-Type CID) Containing One Intra-Molecular Disulfide After Reaction with OH•

Label	CID of $[M+nH+OH]^{n+}$								
	High charge state			Middle charge state			Low charge state		
	Peptide	Charge state	Backbone frag%	Peptide	Charge state	Backbone frag%	Peptide	Charge state	Backbone frag%
1		3+	44		2+	44		1+	33
2		3+	55		2+	46		1+	27
3		2+	88					1+	0
4		3+	25		2+	0		1+	0
5		2+	100					1+	25
6		3+	88		2+	13			
7		2+	75					1+	13
8		2+	71					1+	29
9		3+	85		2+	69			
10		2+	100					1+	33
11		4+	78		3+	100		2+	33

*Only b- and y-types of fragment ions are indicated

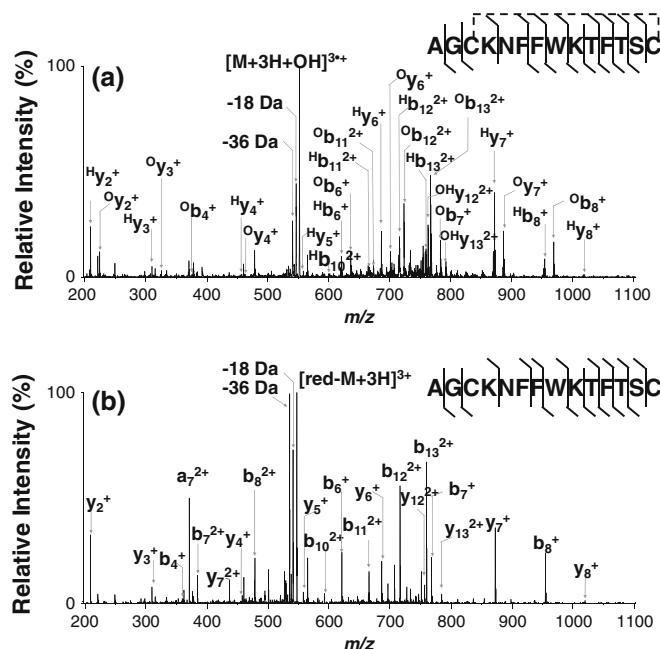


Figure 7. MS² mass spectra derived from Peptide 9 (AGCKNFFWKTFITSC, 3-14 disulfide linkage): (a) beam-type CID of $[M + 3H + OH]^{3+}$ and (b) beam-type CID of $[red - M + 3H]^{3+}$

instance, the observation of $H_{b_{13}}/O_{b_{13}}$ ion pair in Figure 7a suggests that one end of the disulfide bond connects a cysteine at the C-terminus given that Peptide 9 contains 14 amino acid residues. Note that for sequence ions formed outside the disulfide bond loop, they should be observed either with a mass shift of 17 Da (containing both cysteines) or no mass shift (containing no cysteine). Therefore, the presence of $OH_{y_{13}}$ and $OH_{y_{12}}$ ions in Figure 7a indicates those fragmentation sites should be outside the disulfide bond. The backbone fragmentation observed from CID of $[M + nH + OH]^{n+}$ and CID of $[red - M + nH]^{n+}$ is summarized in Table 1S (Supplementary Material) for 11 peptides containing one intra-molecular disulfide bond. The extent of sequence information that can be obtained from each method is represented by backbone frag%. The data clearly show that CID of $[M + nH + OH]^{n+}$ provides similar extent of peptide sequence information to that from CID of disulfide reduced peptide in most cases.

Conclusions

Collisional activation of the OH adduct of peptides containing intramolecular disulfide bonds ($[M + nH + OH]^{n+}$) provides backbone fragments (b- and y-types of ions) within the disulfide loop region, allowing better sequencing capability for disulfide peptides. Due to the formation of sulfenyl radical at the cleavage site, radical initiated side-chain losses, such as losses of 62, 95, and 108 Da, were observed as competitive processes to backbone fragmenta-

tion. We found that charge-directed backbone fragmentation was promoted under beam-type CID conditions and for higher charge states where mobile protons were available. Facile radical-initiated neutral losses were more abundant in ion trap CID of lower charge states. The amount of sequence information obtained from CID of $[M + nH + OH]^{n+}$ ions was similar to that from CID of disulfide bond reduced peptides and could therefore be used as an alternative method for studying disulfide peptides. In addition, coupling on-line OH addition to tandem mass spectrometry has advantages, including (1) simple experimental setup allowing it to be applied to any type of mass spectrometer, (2) reduced sample loss and preparation time due to in situ disulfide bond cleavage followed by mass spectrometry analysis, and (3) potential to be coupled with on-line separation techniques. However, further development is needed to improve the reaction yield and to reduce undesirable side reactions, such as oxidation at peptide side chains.

Acknowledgment

X.M. acknowledges the financial aid by the China Scholarship Council (CSC) to support his research at Purdue University, USA. X.M. and X.Z. also acknowledge the financial support from the National Natural Science Foundation of China (No. 21027013).

References

- Thornton, J.M.: Disulfide bridges in globular-proteins. *J. Mol. Biol.* **151**, 261–287 (1981)
- Gorman, J.J., Wallis, T.P., Pitt, J.J.: Protein disulfide bond determination by mass spectrometry. *Mass Spectrom. Rev.* **21**, 183–216 (2002)
- Lioe, H., Duan, M., O'Hair, R.A.J.: Can metal ions be used as gas-phase disulfide bond cleavage reagents? A survey of coinage metal complexes of model peptides containing an intermolecular disulfide bond. *Rapid Commun. Mass Spectrom.* **21**, 2727–2733 (2007)
- Chrisman, P.A., McLuckey, S.A.: Dissociations of disulfide-linked gaseous polypeptide/protein anions: ion chemistry with implications for protein identification and characterization. *J. Proteome Res.* **1**, 549–557 (2002)
- Zhang, M., Kaltashov, I.A.: Mapping of protein disulfide bonds using negative ion fragmentation with a broadband precursor selection. *Anal. Chem.* **78**, 4820–4829 (2006)
- Bean, M.F., Carr, S.A.: Characterization of disulfide bond position in proteins and sequence-analysis of cystine-bridged peptides by tandem mass-spectrometry. *Anal. Biochem.* **201**, 216–226 (1992)
- Wells, J.M., Stephenson, J.L., McLuckey, S.A.: Charge dependence of protonated insulin decompositions. *Int. J. Mass Spectrom.* **203**, A1–A9 (2000)
- Gunawardena, H.P., O'Hair, R.A.J., McLuckey, S.A.: Selective disulfide bond cleavage in Gold(I) cationized polypeptide ions formed via gas-phase ion/ion cation switching. *J. Proteome Res.* **5**, 2087–2092 (2006)
- Mihalca, R., van der Burgt, Y.E.M., Heck, A.J.R., Heeren, R.M.A.: Disulfide bond cleavages observed in Sori-Cid of three nonapeptides complexed with divalent transition-metal cations. *J. Mass Spectrom.* **42**, 450–458 (2007)
- Kim, H.I., Beauchamp, J.L.: Mapping disulfide bonds in insulin with the route 66 method: selective cleavage of S–C bonds using alkali and alkaline earth metal enolate complexes. *J. Am. Soc. Mass Spectrom.* **20**, 157–166 (2009)
- Kalli, A., Hakansson, K.: Preferential cleavage of S–S and C–S bonds in electron detachment dissociation and infrared multiphoton dissociation.

- tion of disulfide-linked peptide anions. *Int. J. Mass Spectrom.* **263**, 71–81 (2007)
12. Fung, Y.M.E., Kjeldsen, F., Silivra, O.A., Chan, T.W.D., Zubarev, R. A.: Facile disulfide bond cleavage in gaseous peptide and protein cations by ultraviolet photodissociation at 157 Nm. *Angew. Chem. Int. Ed.* **44**, 6399–6403 (2005)
 13. Zubarev, R.A., Kruger, N.A., Fridriksson, E.K., Lewis, M.A., Horn, D. M.: Electron transfer dissociation of multiply protonated and fixed charge disulfide linked polypeptides. *Int. J. Mass Spectrom.* **265**, 130–138 (2007)
 14. Chrisman, P.A., Pitteri, S.J., Hogan, J.M., McLuckey, S.A.: So2-electron transfer ion/ion reactions with disulfide linked polypeptide ions. *J. Am. Soc. Mass Spectrom.* **16**, 1020–1030 (2005)
 15. Gunawardena, H.P., Gorenstein, L., Erickson, D.E., Xia, Y., McLuckey, S. A.: Electron transfer dissociation of multiply protonated and fixed charge disulfide linked polypeptides. *Int. J. Mass Spectrom.* **265**, 130–138 (2007)
 16. Mentinova, M., Han, H., McLuckey, S.A.: Dissociation of disulfide-intact somatostatin ions: the roles of ion type and dissociation method. *Rapid Commun. Mass Spectrom.* **23**, 2647–2655 (2009)
 17. Xia, Y., Cooks, R.G.: Plasma induced oxidative cleavage of disulfide bonds in polypeptides during nanoelectrospray ionization. *Anal. Chem.* **82**, 2856–2864 (2010)
 18. Hopkinson, A.C.: Radical cations of amino acids and peptides: structures and stabilities. *Mass Spectrom. Rev.* **28**, 655–671 (2009)
 19. Chu, I.K., Rodriguez, C.F., Lau, T.C., Hopkinson, A.C., Siu, K.W.M.: Molecular radical cations of oligopeptides. *J. Phys. Chem. B* **104**, 3393–3397 (2000)
 20. Barlow, C.K., McFadyen, W.D., O'Hair, R.A.J.: Formation of cationic peptide radicals by gas-phase redox reactions with trivalent chromium, manganese, iron, and cobalt complexes. *J. Am. Chem. Soc.* **127**, 6109–6115 (2005)
 21. Sun, Q., Nelson, H., Ly, T., Stoltz, B.M., Julian, R.R.: Side chain chemistry mediates backbone fragmentation in hydrogen deficient peptide radicals. *J. Proteome Res.* **8**, 958–966 (2008)
 22. Ly, T., Julian, R.R.: Residue-specific radical-directed dissociation of whole proteins in the gas phase. *J. Am. Chem. Soc.* **130**, 351–358 (2008)
 23. Masterson, D.S., Yin, H., Chacon, A., Hachey, D.L., Norris, J.L., Porter, N.A.: Lysine peroxycarbamates: free radical-promoted peptide cleavage. *J. Am. Chem. Soc.* **126**, 720–721 (2003)
 24. Hao, G., Gross, S.S.: Electrospray tandem mass spectrometry analysis of S- and N-nitrosopeptides: facile loss of NO and radical-induced fragmentation. *J. Am. Soc. Mass Spectrom.* **17**, 1725–1730 (2006)
 25. Wee, S., Mortimer, A., Moran, D., Wright, A., Barlow, C.K., O'Hair, R.A.J., Radom, L., Easton, C.J.: Gas-phase regiocontrolled generation of charged amino acid and peptide radicals. *Chem. Commun.* 4233–4235 (2006)
 26. Kjeldsen, F., Silivra, O.A., Ivonin, I.A., Haselmann, K.F., Gorshkov, M., Zubarev, R.A.: C-Alpha-C backbone fragmentation dominates in electron detachment dissociation of gas-phase polypeptide polyanions. *Chem. Eur. J.* **11**, 1803–1812 (2005)
 27. Lam, C.N.W., Chu, I.K.: Formation of anionic peptide radicals in Vacuo. *J. Am. Soc. Mass Spectrom.* **17**, 1249–1257 (2006)
 28. Laskin, J., Yang, Z.B., Lam, C., Chu, I.K.: Charge-remote fragmentation of odd-electron peptide ions. *Anal. Chem.* **79**, 6607–6614 (2007)
 29. Wee, S., O'Hair, R.A.J., McFadyen, W.D.: The role of the position of the basic residue in the generation and fragmentation of peptide radical cations. *Int. J. Mass Spectrom.* **249**, 171–183 (2006)
 30. Karnezis, A., Barlow, C.K., O'Hair, R.A.J., McFadyen, W.D.: Peptide derivatization as a strategy to form fixed-charge peptide radicals. *Rapid Commun. Mass Spectrom.* **20**, 2865–2870 (2006)
 31. Zubarev, R.A., Kelleher, N.L., McLafferty, F.W.: Electron capture dissociation of multiply charged protein cations. A nonergodic process. *J. Am. Chem. Soc.* **120**, 3265–3266 (1998)
 32. Coon, J.J., Syka, J.E.P., Schwartz, J.C., Shabanowitz, J., Hunt, D.F.: Anion dependence in the partitioning between proton and electron transfer in ion/ion reactions. *Int. J. Mass Spectrom.* **236**, 33–42 (2004)
 33. Syka, J.E.P., Coon, J.J., Schroeder, M.J., Shabanowitz, J., Hunt, D.F.: Peptide and protein sequence analysis by electron transfer dissociation mass spectrometry. *Proc. Natl. Acad. Sci. U. S. A.* **101**, 9528–9533 (2004)
 34. Turecek, F.: N–C–Alpha bond dissociation energies and kinetics in amide and peptide radicals. Is the dissociation a non-ergodic process? *J. Am. Chem. Soc.* **125**, 5954–5963 (2003)
 35. Zubarev, R.A., Haselmann, K.F., Budnik, B., Kjeldsen, F., Jensen, F.: Towards an understanding of the mechanism of electron-capture dissociation: a historical perspective and modern ideas. *Eur. J. Mass Spectrom.* **8**, 337–349 (2002)
 36. Sobczyk, M., Anusiewicz, W., Berdys-Kochanska, J., Sawicka, A., Skurski, P., Simons, J.: Coulomb-assisted dissociative electron attachment: application to a model peptide. *J. Phys. Chem. A* **109**, 250–258 (2005)
 37. Hager, J.W.A.: New linear ion trap mass spectrometer. *Rapid Commun. Mass Spectrom.* **16**, 512–526 (2002)
 38. Sankaranarayanan, R., Pashaie, B., Dhali, S.K.: Laser-induced fluorescence of OH radicals in a dielectric barrier discharge. *Appl. Phys. Lett.* **77**, 2970–2972 (2000)
 39. Lioe, H., O'Hair, R.A.J.: A novel salt bridge mechanism highlights the need for nonmobile proton conditions to promote disulfide bond cleavage in protonated peptides under low-energy collisional activation. *J. Am. Soc. Mass Spectrom.* **18**, 1109–1123 (2007)
 40. Turecek, F., Syrtstad, E.A.: Mechanism and energetics of intramolecular hydrogen transfer in amide and peptide radicals and cation-radicals. *J. Am. Chem. Soc.* **125**, 3353–3369 (2003)
 41. Leymarie, N., Costello, C.E., O'Connor, P.B.: Electron capture dissociation initiates a free radical reaction cascade. *J. Am. Chem. Soc.* **125**, 8949–8958 (2003)
 42. Li, X., Lin, C., Han, L., Costello, C.E., O'Connor, P.B.: Charge remote fragmentation in electron capture and electron transfer dissociation. *J. Am. Soc. Mass Spectrom.* **21**, 646–656 (2010)
 43. Fung, Y.M.E., Chan, T.W.D.: Experimental and theoretical investigations of the loss of amino acid side chains in electron capture dissociation of model peptides. *J. Am. Soc. Mass Spectrom.* **16**, 1523–1535 (2005)
 44. Han, H.L., Xia, Y., McLuckey, S.A.: Ion trap collisional activation of C and Z' ions formed via gas-phase ion/ion electron-transfer dissociation. *J. Proteome Res.* **6**, 3062–3069 (2007)
 45. McLuckey, S.A.: Principles of collisional activation in analytical mass-spectrometry. *J. Am. Soc. Mass Spectrom.* **3**, 599–614 (1992)
 46. McLuckey, S.A., Goeringer, D.E.: Slow heating methods in tandem mass spectrometry. *J. Mass Spectrom.* **32**, 461–474 (1997)
 47. Paizs, B., Suhai, S.: Fragmentation pathways of protonated peptides. *Mass Spectrom. Rev.* **24**, 508–548 (2005)
 48. Wysocki, V.H., Tsaprailis, G., Smith, L.L., Brei, L.A.: Mobile and localized protons: a framework for understanding peptide dissociation. *J. Mass Spectrom.* **35**, 1399–1406 (2000)